Korean J. Chem. Eng., 34(3), 706-716 (2017)
DOI: 10.1007/s11814-016-0318-9

pISSN: 0256-1115
eISSN: 1975-7220

A new approach for modeling of multicomponent gas hydrate formation

Vahid Mohebbi*,†, Reza Mosayyebi Behbahani*, and Abbas Naderifar**

*Gas Engineering Department, Petroleum University of Technology, Iran
**Chemical Engineering Department, Amirkabir University of Technology, Iran
(*Received 22 July 2016 • accepted 10 November 2016*)

Abstract−Several models have been proposed to investigate the kinetics of gas hydrate formation. The main differences between the proposed models are the definition of the driving force, thermodynamics approach and the number of resistances to study the gas consumption by the hydrate phase. This paper concentrates on gas hydrate formation from multicomponent mixture, which has not been much studied before. In the present research, chemical potential has been considered as the driving force and, consequently, a new resistance coefficient was introduced. A complete discussion and reasonable assumptions has been provided to support this modelling.

Keywords: Gas Hydrates, Natural Gas, Multicomponent, Driving Force, Kinetics, Thermodynamics

INTRODUCTION

Gas hydrates are a set of clathrates formed from the combination of water and certain gases under conditions of high pressure and low temperature. The hydrate structure is stabilized when gas molecules occupy "cages" formed by hydrogen-bonded water molecules. Interest in these compounds has risen in recent years due to the discovery of large deposits below the ocean floor and in permafrost regions [1]. Hydrates have important applications in many areas, including flow assurance of oil and gas lines, potential sources of natural gas (mostly methane) from permafrost and deep-sea hydrate deposits, and energy storage and transportation [2]. Hydrate formation is a major issue as far as the flow assurance of oil and gas lines is concerned. The oil and gas industry spends over $200 million annually to prevent hydrate formation and maintain flow assurance [3]. Today, several applications have been proposed that have rendered the gas hydrate phenomenon as a novel technique. The application of gas hydrates in carbon dioxide sequestration, separation processes, and natural-gas storage and transportation has intrigued many researchers over the past years [4]. Moreover, huge sources of natural-gas hydrate have been discovered, and considerable efforts have been made towards the production of this type of resource [5]. Understanding the kinetics of hydrate formation is necessary insofar as the mentioned applications are concerned. Several researchers have attempted to discover and predict hydrate formation. Vysniauskas and Bishnoi were the first to measure the rate of methane hydrate formation [6].

Based on crystallization kinetic and mass transfer effect, Englezos et al. developed a model to predict the formation kinetics of methane and ethane hydrates [7]. Gillard et al. proposed an empirical correlation based on the work by Englezos et al [8]. Monfort et al. also proposed a semi-empirical model with fugacity and driving force taken from Englezos et al. and Vysniauskas and Bishnoi, respectively [9]. According to Clarke and Bishnoi, the model by Englezos et al. is only valid for low supersaturating systems due to the assumption of negligible primary crystallization after nucleation [10]. Zhang et al. used the proposed model by Englezos et al. and applied it for methane hydrate formation in the presence of sodium dodecyl sulfate [11]. Skovberg and Rasmussen simplified Englezos' model to mass transfer limited model, where they assumed that the most important step in gas diffusion through water is gas-liquid interface mass transfer, which controls the hydrate formation kinetics [12]. Most of the theoretical and experimental studies were carried out to reveal that hydrate formation and growth mechanism were inherently system-dependent.

Depending on the approach to model the behavior of the gas hydrate formation (or dissociation), the appropriate driving force has been selected by researchers. In this paper, the mass transfer approach was employed to model multicomponent gas hydrate formation. In this manner, chemical potential was selected as the driving force [13], and was implemented for the case of multicomponent mixture. A complete discussion and reasonable assumptions has been provided for this purpose.

APPROACHES TO PREDICT GAS HYDRATE KINETICS

As the gas hydrate formation (or dissociation) process deals with heat and mass transfer, including several resistances, most researchers prefer to emphasize one or some of these resistances and approaches. As the temperature is kept constant in most of the experiments, thermal resistance is ignored in many studies, although there have been some considerable attempts to assume the gas hydrate formation (or dissociation) as the thermal process. In the current study, an isothermal process was assumed. Consequently, thermal resistance was omitted. Three main approaches are available in the literature as briefly described here.

†To whom correspondence should be addressed.
E-mail: mohebbi@put.ac.ir

1. Bishnoi and Vysniauskas' Semi-empirical Model

Bishnoi and Vysniauskas analyzed methane hydrate formation in a stirred semi-batch reactor operating at constant pressure. A three-step reaction mechanism was postulated and subsequently utilized for the formulation of a semi-empirical equation for computing the methane consumption rate [6]:

$$(dn/dt) = \alpha \times A_{A-L} \times e^{-\frac{E_a}{RT}} \times e^{\frac{-a}{(T_{EQ}-T)^b}} \times P^{\gamma} \quad (1)$$

where, α, a, b, E_a, and γ should be experimentally determined.

2. The Intrinsic Model by Englezos et al.

Englezos et al. conducted some experiments about the formation of methane and ethane hydrates and developed a combined model of mass transfer and crystallization [7]. According to their model, hydrate formation is composed of three steps:

1. Diffusion of guest molecules from gas-liquid interface to liquid bulk,

2. Diffusion of guest molecules from the liquid bulk to hydrate-solution interface,

3. Reaction of water and guest molecule at the hydrate-solid interface.

The driving force for hydrate formation was defined as the difference between the fugacity of the dissolved gas and the equilibrium fugacity at the experimental temperature [7].

$$(dn/dt)_{Particle} = K^* A_{Particle}(f - f_{EQ}) \quad (2)$$

3. The Model of Skovberg-Rasmussen-mass Transfer Approach

Based on their analysis of the model by Englezos et al. [7], Skovberg and Rasmussen [12] proposed its simplification, removing PBE and assuming that all resistances to mass transfer during hydrate formation lay in the diffusion of the dissolved gas from the gas-liquid interface to the liquid bulk [14]. Thus, in their formulation, the gas consumption rate is given by:

$$dn/dt = k_L A_{V-L} C_W (x_I - x_B) \quad (3)$$

Mohebbi et al. utilized the concept of Skovberg and Rasmussen's model, which can predict the current experimental data in CSTR reactors [15]. They did several experiments on methane to prove their idea. They also used the concentration as the driving force. The main difference between their model and that proposed by Skovberg and Rasmussen is that they assume that the solubility in the bulk of the liquid is at equilibrium pressure and operating temperature.

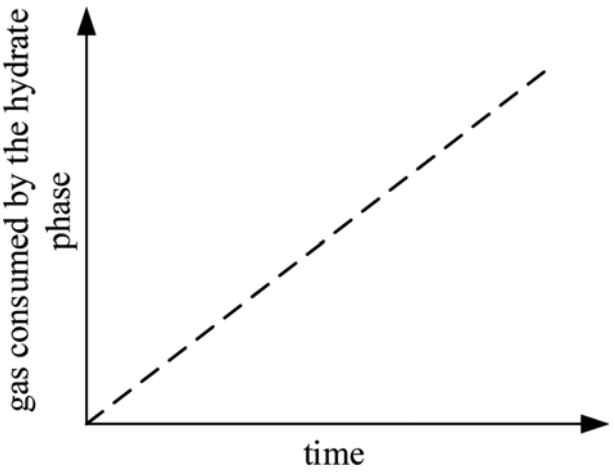

Fig. 1. Schematic diagram of constant gas conumption rate.

There are two explanations to evaluate the mass transfer approach models:

3-1. Constant Rate of Gas Consumption

Table 1 shows the previous works in which the rate of gas uptake is constant. A schematic illustration is presented in Fig. 1. The gas consumption rate is conserved at an initial stage of gas hydrate formation. After this stage, considerable amount of solid hydrates is accumulated in the interface which reduces the contact area and increases the diffusion resistance considerably. The decrease in contact area and increase of mass transfer resistance may be responsible for the reduction of gas consumption rate as it was previously measured by Lee et al. and Zhang et al. [11,16].

Because all physical parameters of experiments are kept constant during experiments (initial stage) and only parameters related to hydrate growth vary with time, it is reasonable to ignore the changing parameters in comparison with mass transfer in the gas-liquid interface.

3-2. Constant Gas Mole Fraction in the Aqueous Phase

In the mass transfer approach, it is assumed that the kinetic of

Table 1. Previous works in which the gas consumption has linear trend with respect to time

Researchers (s)	Component	Reference
Vysniauskas and Bishnoi	Methane	[6]
Englezos et al.	Methane, Ethane	[7]
Chum and Lee	Carbon Dioxide	[17]
Malegaonkar et al.	Methane, Carbon Dioxide	[18]
Bergeron and Servio	Propane	[19]
Bergeron et al.	Methane	[20]
Lee et al.	Methane (in sodium dodecyl sulfate solution)	[16]
Zhang et al.	Methane (in sodium dodecyl sulfate solution)	[11]
Zhang et al.	Carbon Dioxide	[21]
Mohebbi et al.	Methane	[15]
Naseh et al.	Ethane	[22]

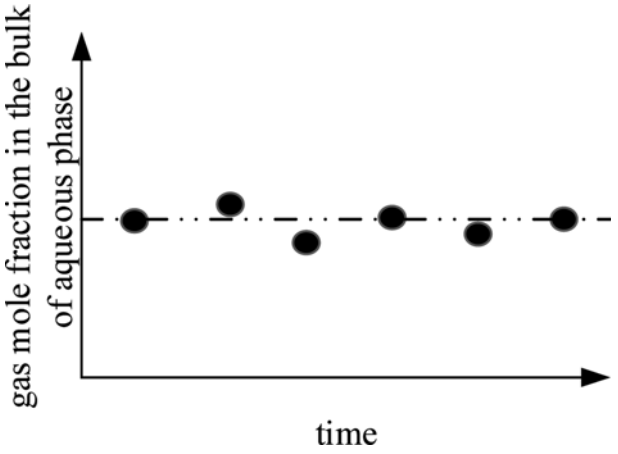

Fig. 2. Constant mole fraction of gas compounds in the aqueous phase during hydrate formation.

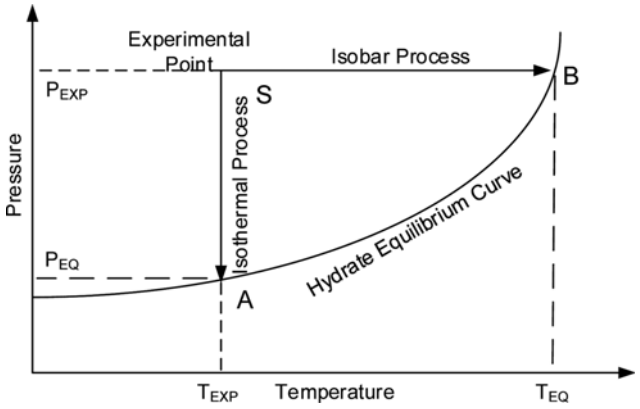

Fig. 3. Isobaric and isothermal process during gas hydrate formation.

gas hydrate particle is negligible compared to the mass transfer in the gas-liquid interface. This means that all liquid properties, including guest molecule composition in the bulk of liquid are constant (as demonstrated by Fig. 2). There are some reports experimentally stating the mole fraction of soluble gas in water during hydrate formation [23,24].

The advantage of the mass transfer approach (which has been applied in this study) is extensibility for multicomponent systems by the following expression:

$$dn/dt = A_{A-L} C_W \Sigma_{i=1}^{m} k_L^i (x_I^i - x_B^i) \quad (4)$$

DRIVING FORCE

1. Previous Works

Driving force is essential to transfer component(s) from one phase to another. Consequently, at equilibrium conditions, there is no driving force between the phases. The mass transfer coefficient is defined as the ratio of mass transfer rate and the driving force.

Different types of the driving force have been introduced to study the formation (dissociation) of gas hydrates. Vysniauskas and Bishnoi utilized the difference between temperatures at experimental and equilibrium conditions as the driving force [6]. This type of experiment has by Izadpanah et al. [25]. In addition, Peng et al. used the degree of subcooling as the driving force to study the hydrate film growth on the surface of a gas bubble suspended in water [26]. Englezos et al. used the fugacity as the driving force as the first time [7]. This driving force was used by some researchers later [27,28]. Skovberg and Rasmussen used the concentration (mole fraction) in their work [12]. Sloan and Christiansen assumed the Gibbs free energy as the driving force [29], while Firoozabadi and Kashchiev used the chemical potential function [13].

To have a better concept of the driving force, it is worth introducing two types of process, isothermal and isobaric. The idea of isobaric and isothermal approaches was cited before by Kashchiev and Firoozabadi [13]. They did a comprehensive study on the driving force in case of single component gas hydrate formation. The present work is concentrated on the multicomponent systems while introducing a new mass transfer coefficient that is independent of the composition in the gas phase.

In the isobaric regime, it is assumed that the system condition (S) is compared to its corresponding equilibrium point (B) at constant pressure (see Fig. 3). Similarly, in the isothermal process, the driving force is varied by changing the pressure. In this regime, the experimental point varies in line AS, and the driving force is defined based upon the difference between points A and S.

According to selection of one of these two concepts, MTC k_L can be determined straightforwardly. If an isobar process is assumed (SB), the bulk liquid concentration (CB) is defined at point B. Otherwise, if an isothermal process is chosen, CB is defined at point A. In both approaches, the liquid phase concentration changes rapidly to its corresponding state at equilibrium conditions as hydrate formation occurs. The isothermal process was used in the current study.

2. Comprehensive Analysis

As previously stated, the difference between mole fractions of guest molecules was defined as the driving force to form or dissociate gas hydrate. From the viewpoint of thermodynamics, the difference between chemical potential between phases is responsible for formation or dissociation. In a general case, the guest molecules diffuse from the gas phase and form solid phase (we have assumed that the guest molecules are present in the gas phase in

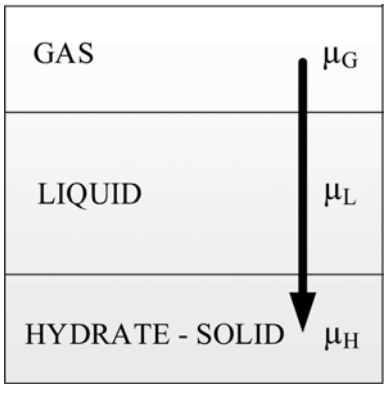

Fig. 4. Representative of gas diffusion direction.

the contact of the aqueous phase in this study). Fig. 4 indicates the conceptual contacts of three phases.

μ_G, μ_L, and μ_H are chemical potentials in gas, liquid (aqueous phase), and hydrate, respectively. Therefore, the general driving force can be written as:

$$\Delta\mu=\mu_G-\mu_H \tag{5}$$

In this research, we have considered four approaches to investigate the driving force:

1. Equilibrium between liquid and hydrate, while no equilibrium exists between gas and liquid.
2. Equilibrium between gas and liquid, while no equilibrium is present between liquid and hydrate.
3. No equilibrium is observed between all phases.
4. Existence of hydrate in non-equilibrium conditions (no movement from point B to A in Fig. 3).

2-1. Equilibrium between Liquid and Hydrate

Assume that there are equilibrium conditions between liquid and gas hydrate phases. Thus, the driving force (Eq. (5)) can be rewritten as:

$$\Delta\mu=\mu_G-\mu_L \tag{6}$$

If there are "m" components in the gas phase (excluding water), the total chemical potential for the gas phase in the operating temperature and pressure is:

$$\mu_G=\mu_G^0+\mathrm{RT}\Sigma_{i=1}^{m}y^i\ln f_G^i \tag{7}$$

It is supposed that the mixture of liquid (water) and gas hydrate moves from super-saturation to equilibrium conditions (operating temperature and corresponding equilibrium pressure). Accordingly, the liquid chemical potential can be presented by:

$$\mu_L=\mu_{L.P_{EQ}}^{Gas}+\mu_{L.P_{EQ}}^{W} \tag{8}$$

or

$$\mu_L=\mu_L^0+\mathrm{RT}\Sigma_{i=1}^{m}x_{P_{EQ}}^i\ln f_{G.P_{EQ}}^i+(1-\Sigma_{i=1}^{m}x^i)\int_0^{P_{EQ}}v^W dP' \tag{9}$$

where, $x_{P_{EQ}}^i$ and v^W are mole fractions of component i in water at equilibrium pressure and water molar volume, respectively. The equilibrium pressure can be predicted, using an appropriate thermodynamic model (Appendix A). Substitution of Eqs. (7) and (9) in Eq. (6) yields:

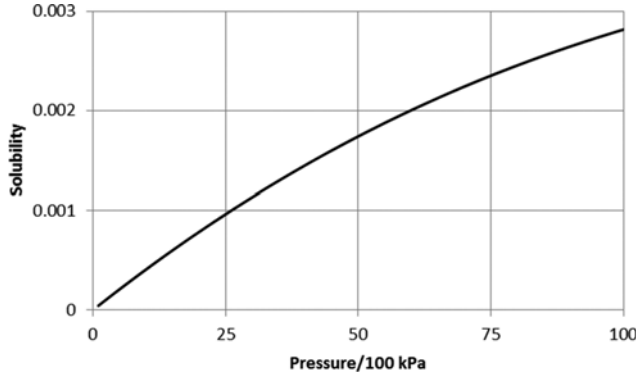

Fig. 5. Methane solubility in water at 273.2 K.

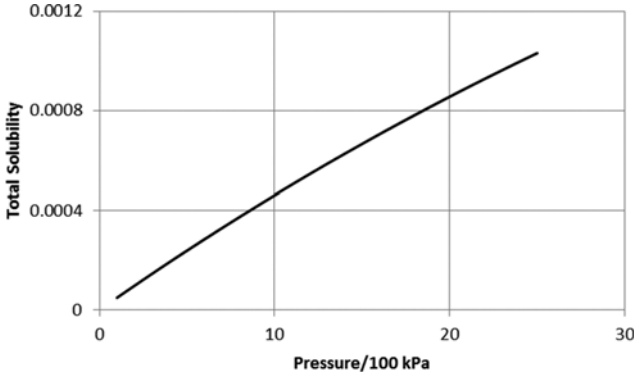

Fig. 6. Total solubility of a natural gas mixture in water at 273.2 K.

Table 2. Composition of natural gas mixture used in Fig. 6

Mole percent	Material
75	Methane
12	Ethane
8	Propane
5	i-Butane

$$\Delta\mu=\mu_G^0-\mu_L^0+\mathrm{RT}\Sigma_{i=1}^{m}y^i\ln f_G^i-\mathrm{RT}\Sigma_{i=1}^{m}x_{P_{EQ}}^i\ln f_{G.P_{EQ}}^i-(1-\Sigma_{i=1}^{m}x^i)\int_0^{P_{EQ}}v^W dP' \tag{10}$$

Since the solubility of guest gases in water is very low, it is reasonable to ignore the gas solubility in water. To show this idea, the solubility of methane and a gas mixture in water at 273.2 K is illustrated in Figs. 5 and 6. The composition of the natural-gas mixture is tabulated in Table 2. Henry's law has been used to predict the solubility at low temperatures [30].

Thus, Eq. (10) is expressed as:

$$\Delta\mu=\mu_G^0-\mu_L^0+\mathrm{RT}\Sigma_{i=1}^{m}y^i\ln f_G^i-\int_0^{P_{EQ}}v^W dP'-\mathrm{RT}\Sigma_{i=1}^{m}x_{P_{EQ}}^i\ln f_{G.P_{EQ}}^i \tag{11}$$

At equilibrium pressure, the driving force is equal to zero, and the above equation is converted as follows:

$$0=\mu_G^0-\mu_L^0+\mathrm{RT}\Sigma_{i=1}^{m}y^i\ln f_{G.P_{EQ}}^i-\int_0^{P_{EQ}}v_L^W dP'-\mathrm{RT}\Sigma_{i=1}^{m}x_{P_{EQ}}^i\ln f_{G.P_{EQ}}^i \tag{12}$$

Subtracting these equations yields:

$$\Delta\mu=\mathrm{RT}\Sigma_{i=1}^{m}y^i\ln f_G^i/f_{G.P_{EQ}}^i \tag{13}$$

The general mass transfer coefficient (GMTC) can be defined according to Eq. (13):

$$K_\mu=(dn_H/dt)/A_{V-L}\mathrm{RT}\Sigma_{i=1}^{m}y^i\ln f_G^i/f_{G.P_{EQ}}^i \tag{14}$$

and the total gas consumption can be predicted as:

$$dn_H/dt=A_{V-L}K_\mu\mathrm{RT}\Sigma_{i=1}^{m}y^i\ln f_G^i/f_{G.P_{EQ}}^i \tag{15}$$

GMTC can be determined experimentally. If f_G^i is relatively close to $f_{G.P_{EQ}}^i$, the above equation will be approximated as:

$$dn_H/dt=A_{V-L}K_\mu\mathrm{RT}\Sigma_{i=1}^{m}y^i(f_G^i/f_{G.P_{EQ}}^i-1) \tag{16}$$

or

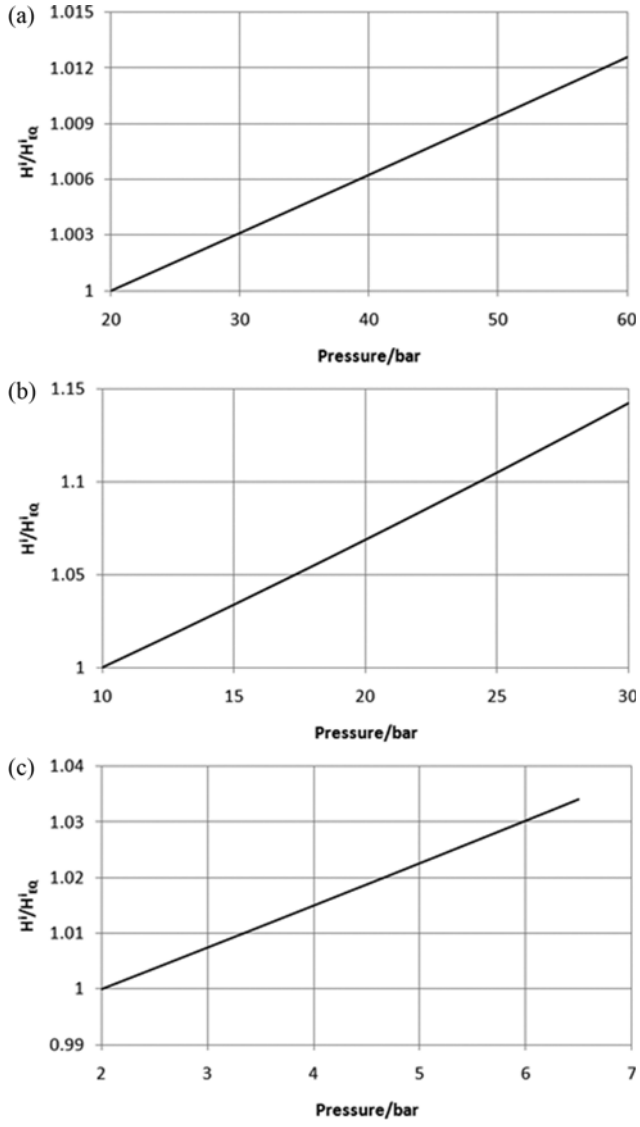

Fig. 7. The ratio of Henry's law constant: (a) Methane at 275 K, (b) ethane at 285 K, (c) propane at 285 K.

$$dn_H/dt = A_{V-L}K_\mu RT\Sigma_{i=1}^{m} y^i(H^i x^i/H_{EQ}^i x_{EQ}^i - 1) \tag{17}$$

where H is Henry's law constant and H^i and H_{EQ}^i are both at operating temperature, but the former is at operating pressure, and the latter is at the corresponding equilibrium pressure. Henry's law constant depends on temperature and is a weak function of pressure. Consequently, H^i/H_{EQ}^i is relatively close to unity. Fig. 7 illustrates that this assumption is valid.

Eq. (17) can be represented as follows:

$$dn_H/dt = A_{V-L}C_W\Sigma_{i=1}^{m}(K_\mu RTy^i/C_W x_{EQ}^i)(x^i - x_{EQ}^i) \tag{18}$$

which is similar to Eq. (4). The mass transfer coefficient for each component can be determined according to the following relation:

$$k_L^i = K_\mu RTy^i/C_W x_{EQ}^i \tag{19}$$

2-2. Equilibrium between Gas and Aqueous Phases

In this approach, we assume that the gas and aqueous phases are in equilibrium, and the reason for mass transfer is the difference in chemical potential between the aqueous and hydrate phases, which can be described as follows:

$$\Delta\mu = \mu_L^{Gas} + n_W\mu_L^W - \mu_H \tag{20}$$

where, n_W is the hydration number. It has been assumed that the hydrate phase can move from super-saturation condition to isothermal equilibrium conditions. Thus, Eq. (20) can be well presented by:

$$\Delta\mu = \mu_{L.P}^{Gas} + n_W\mu_{L.P}^W - \mu_{H.P_{EQ}} \tag{21}$$

where,

$$\mu_{L.P}^{Gas} = \mu_{G.P}^{Gas} = \mu_G^{Gas.0} + RT\Sigma_{i=1}^{m} y^i \ln f_{G.P}^i \tag{22}$$

$$\mu_{L.P}^W = \mu_L^{W.0} + \int_0^P v_L^W dP' \tag{23}$$

$$\mu_{H.P_{EQ}} = \mu_H^0 + \int_0^{P_{EQ}} v_H dP' \tag{24}$$

Substituting Eqs. (22)-(24) in Eq. (21) yields:

$$\Delta\mu = \mu_G^{Gas.0} + RT\Sigma_{i=1}^{m} y^i \ln f_{G.P}^i + n_W\left(\mu_L^{W.0} + \int_0^P v_L^W dP'\right) - \mu_H^0 - \int_0^{P_{EQ}} v_H dP' \tag{25}$$

In equilibrium conditions, $\Delta\mu$ approaches zero and we have:

$$0 = \mu_G^{Gas.0} + RT\Sigma_{i=1}^{m} y^i \ln f_{G.P_{EQ}}^i + n_W\left(\mu_L^{W.0} + \int_0^{P_{EQ}} v_L^W dP'\right) - \mu_H^0 - \int_0^{P_{EQ}} v_H dP' \tag{26}$$

By subtracting Eq. (26) from Eq. (25), the driving force in this method can be expressed by:

$$\Delta\mu = RT\Sigma_{i=1}^{m} y^i \ln f_{G.P}^i/f_{G.P_{EQ}}^i + n_W v_L^W(P - P_{EQ}) \tag{27}$$

There are two terms contributing in the above equation, gas and water terms. In the following examples, the magnitude of the water term in the driving force will be explained.

2-2-1. Example 1: Methane Hydrate Formation

Assume methane hydrate formation process in 273.2 K. The equilibrium pressure at this temperature is close to 27 bar. The operating pressure varies from 27 to 105 bar, and the driving force is plotted against the pressure in Fig. 8. The continuous curve presents the dimensionless driving force by considering the effect of water term (the second term on the right side of Eq. (27)), while the dashed curve is the driving force, which ignores the effect of water in the definition of the driving force. In the current study, SRK EOS [31] was implemented to estimate the fugacity (fugacity coefficient) and compressibility factor. In the case of gas mixture, the binary interaction coefficients are reported in the Appendix [32].

As can be seen, the importance of the 'water term' in the driving force is negligible close to equilibrium pressure, and the magnitude of this term will rise by increasing the pressure. In most situations, there is a difference between operating and equilibrium pressures that is not so considerable. Consequently, it is reasonable to ignore this term in comparison to the gas term.

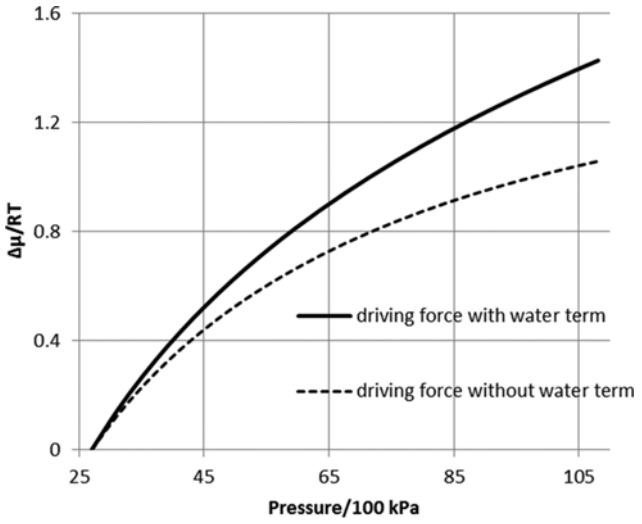

Fig. 8. Driving force during methane hydrate formation with and without water term (Eq. (27)) at 273.2 K.

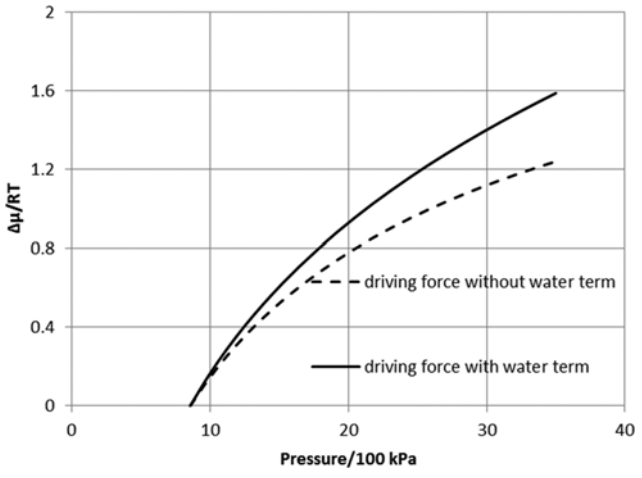

Fig. 9. Driving force during gas mixture hydrate formation with and without water term (Eq. (27)) at 280 K.

2-2-2. Example 2: Hydrate Formation from a Gas Mixture

The natural-gas mixture (Table 2) is investigated at 280 K in this part. The pressure differs between equilibrium and dew-point pressures (8.6 to 35.4 bar). Fig. 9 shows the chemical potential variation with pressure. The continuous curve illustrates the dependency of chemical potential on pressure by considering the effect of the water term, whereas the dashed curve ignores this dependency. The difference between the two assumptions can be ignored at pressure close to equilibrium pressure. At elevated pressure, this difference is considerable. Thus, the water term can be ignored at a pressure close to equilibrium pressure.

Accordingly, at pressure close to equilibrium pressure, the driving force can be written as follows:

$$\Delta\mu = RT\Sigma_{i=1}^{m} y^i \ln f_{G.P}^i / f_{G.P_{EQ}}^i \tag{28}$$

Similar to Eq. (18), the equation of gas consumption with the hydrate phase is:

$$\begin{aligned} dn_H/dt &= A_{V-L} K_\mu RT\Sigma_{i=1}^{m} y^i \ln f_{G.P}^i / f_{G.P_{EQ}}^i \\ &= A_{V-L} C_W \Sigma_{i=1}^{m} (K_\mu RT y^i / C_W x_{EQ}^i)(x^i - x_{EQ}^i) \end{aligned} \tag{29}$$

Comparing the above equation and Eq. (4) yields:

$$k_L^i = K_\mu RT y^i / C_W x_{EQ}^i \tag{30}$$

2-3. Non-equilibrium Conditions between All Phases

In previous sections, we assumed that there may be equilibrium conditions between the two phases. Now we assume no equilibrium between phases. In this case, the driving force can be selected as the difference between initial compounds (gas and water molecules) and hydrate phase:

$$\Delta\mu = \mu_{Reactants} - \mu_{Product} = \mu_{G.P}^{Gas} + n_W \mu_{L.P}^{W} - \mu_{H.P_{EQ}} \tag{31}$$

or

$$\begin{aligned} \Delta\mu = \mu_G^{Gas.0} + RT\Sigma_{i=1}^{m} y^i \ln f_{G.P}^i + n_W \left(\mu_L^{W.0} + \int_0^P v_L^W dP' \right) \\ - \mu_H^0 - \int_0^{P_{EQ}} v_H dP' \end{aligned} \tag{32}$$

In equilibrium point:

$$\begin{aligned} 0 = \mu_G^{Gas.0} + RT\Sigma_{i=1}^{m} y^i \ln f_{G.P_{EQ}}^i + n_W \left(\mu_L^{W.0} + \int_0^{P_{EQ}} v_L^W dP' \right) \\ - \mu_H^0 - \int_0^{P_{EQ}} v_H dP' \end{aligned} \tag{33}$$

Subtracting the above two equations yields:

$$\Delta\mu = \mu_G - \mu_H = RT\Sigma_{i=1}^{m} y^i \ln f_{G.P}^i / f_{G.P_{EQ}}^i \tag{34}$$

which is similar to Eq. (28).

2-4. General Approach

Earlier, we assumed that the hydrate phase moves from supersaturation conditions to equilibrium conditions. In the current approach, this assumption is no longer valid. Thus, the gas hydrate point does not move from its initial point to point S (see Fig. 3). Similar to the aforementioned modelling, the driving force can be written as:

$$\begin{aligned} \Delta\mu = \mu_G^{Gas.0} + RT\Sigma_{i=1}^{m} y^i \ln f_{G.P}^i + n_W \left(\mu_L^{W.0} + \int_0^P v_L^W dP' \right) \\ - \mu_H^0 - \int_0^P v_H dP' \end{aligned} \tag{35}$$

At equilibrium point we have:

$$\begin{aligned} 0 = \mu_G^{Gas.0} + RT\Sigma_{i=1}^{m} y^i \ln f_{G.P_{EQ}}^i + n_W \left(\mu_L^{W.0} + \int_0^{P_{EQ}} v_L^W dP' \right) \\ - \mu_H^0 - \int_0^{P_{EQ}} v_H dP' \end{aligned} \tag{36}$$

Subtracting the two above equations yields:

$$\Delta\mu = RT\Sigma_{i=1}^{m} y^i \ln f_{G.P}^i / f_{G.P_{EQ}}^i + n_W \int_{P_{EQ}}^{P} v_L^W dP' - \int_{P_{EQ}}^{P} v_H dP' \tag{37}$$

If the functionality of specific volume of water and hydrate on pressure is negligible, we have:

$$\Delta\mu = RT\Sigma_{i=1}^{m} y^i \ln f_{G.P}^i / f_{G.P_{EQ}}^i + (n_W v_L^W - v_H)(P - P_{EQ}) \tag{38}$$

Similar to previous approaches, the second term in the right side of Eq. (38) can be ignored compared with the first term.

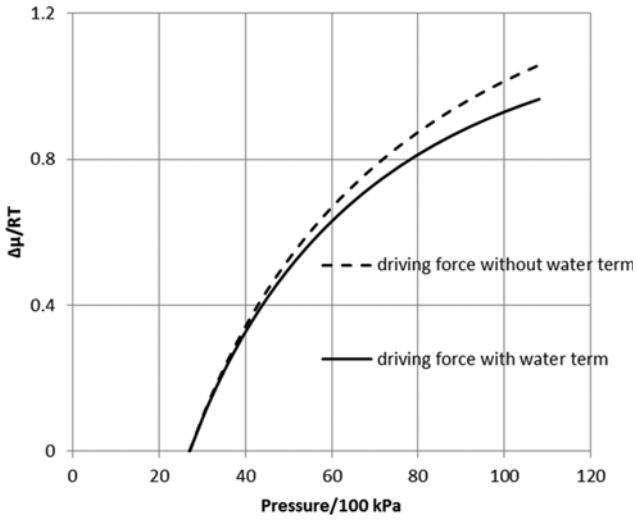

Fig. 10. Driving force during gas hydrate formation of methane at 273.2 K.

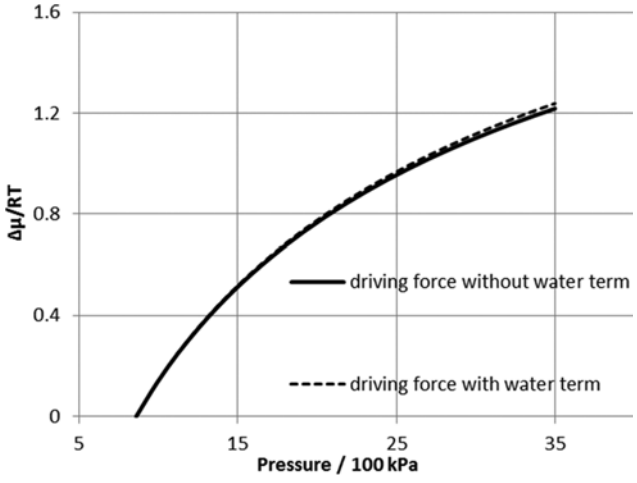

Fig. 11. Driving force during gas hydrate formation from gas mixture (Table 2) at 280 K.

$$\Delta\mu = RT\Sigma_{i=1}^{m} y^i \ln f_{G.P}^i / f_{G.P_{EQ}}^i \quad (39)$$

Similar to section 3.2.2, Eqs. (38) and (39) were compared to the case of methane and natural-gas mixture (Table 2). Figs. 10 and 11 present both equations for methane and gas mixture at 273.2 K and 280 K, respectively. As it was predictable, the difference between the equations is negligible in the pressure close to equilibrium pressures. Hence, selecting Eq. (39) as the driving force is acceptable.

Similar to Eq. (14), the general mass transfer coefficient can be defined as:

$$K_\mu = (dn_H/dt)/A_{V-L} RT\Sigma_{i=1}^{m} y^i \ln f_G^i / f_{G.P_{EQ}}^i \quad (40)$$

2-5. Other Types of Driving Forces

Eq. (39) can be converted to the following equation in the case of single component:

$$\Delta\mu = RT \ln f_{G.P}/f_{G.P_{EQ}} \quad (41)$$

If the fugacity ratio is relatively close to unity, the driving force will be:

$$\Delta\mu = RT(f_{G.P}/f_{G.P_{EQ}} - 1) = \frac{RT}{f_{G.P_{EQ}}}(f_{G.P} - f_{G.P_{EQ}}) = \alpha(f_{G.P} - f_{G.P_{EQ}}) \quad (43)$$

where, α is constant at fixed temperature. The above equation indicates that the fugacity can be used as an alternative of chemical potential, which has been used by several researchers [7,17,18].

The fugacity is the multiple of pressure and fugacity coefficient. Thus:

$$\Delta\mu = \alpha(f_{G.P} - f_{G.P_{EQ}}) = \alpha(\varphi_{G.P}P - \varphi_{G.P_{EQ}}P_{EQ}) \quad (44)$$

where, $\varphi_{G.P}$ and $\varphi_{G.P_{EQ}}$ are fugacity coefficients in operating and equilibrium pressures, respectively. Once again, if operating and equilibrium pressures are not so much different, it is reasonable to assume that both fugacity coefficients are the same and we have:

$$\Delta\mu = \alpha\varphi_{G.P_{EQ}}(P - P_{EQ}) = \beta(P - P_{EQ}) \quad (45)$$

Eq. (45) introduces the pressure as the driving force. Although this type of driving force has been obtained with several simplifications, it is a sensible and measurable variable.

PARAMETER EVALUATION

There are several studies in literature about gas hydrate kinetics from single component. Eq. (4), which is based on the mass transfer approach, can predict the rate of gas consumption by the hydrate phase adequately. However, in the present study, we used the research results of Mohebbi and Behbahani, which are about the gas hydrate formation from a natural-gas mixture [33]. The mixture consists of methane, ethane, propane, and isobutene mixture as they contribute during hydrate formation. Temperature and pressure changed from 275.15 K to 287.25 K and 1.1 MPa to 5.4 MPa, respectively. As all experiments were carried out under isothermal conditions, they used the difference between the operating pressure and equilibrium pressure as the driving force. A summary of the experimental data is given in Table 3. In this work, Eqs. (4) and (14) have been used to evaluate general and component mass transfer coefficients, respectively.

Table 3. General conditions of experimental data [33]

Experiment	Temperature/K	Initial and final pressures/100 kPa
1	275.15	11.7-11.0
2	275.15	15.7-15.0
3	275.15	19.8-19.3
4	278.15	14.0-12.9
5	278.15	14.0-13.0
6	278.15	18.2-17.3
7	278.15	24.5-24.0
8	282.95	20.1-19.3
9	282.95	23.7-22.7
10	287.25	39.5-38.8
11	287.25	45.1-44.2
12	287.25	55.5-54.7

Table 4. Unknown parameters of Eq. (4)

Component/Parameter	a	b	c	d	e	R-square
CH_4	13.6	−0.05108	1.217	−0.004063	−0.0001888	0.92
C_2H_6	19.36	−0.07274	0.4229	−0.001185	−0.0005409	0.92
C_3H_8	52.72	−0.196	0.7195	−0.001945	6e-5	0.96
i-C_4H_{10}	168.6	−0.628	2.282	−0.006123	−0.001715	0.88

We found that the component mass transfer coefficient depends on both pressure and temperature. The component mass transfer coefficient (k_L) can be directly determined at different pressures (Eq. (4)). To reduce the number of figures, only three data results of the mentioned experiments are illustrated here. Twelve sets of experimental data were available. Each experiment was executed in isochoric and isothermal conditions. As the pressure varied during experiments, three gas consumption rates were selected and, therefore, 36 sets of data were available. Previously, Mohebbi et al. showed that the kinetics of gas hydrate in isochoric and isobaric experiments has the same behavior [15].

Accordingly, a polynomial correlation was introduced which well presents this dependency.

$$k_L^i = 10^{-4}(a^i + b^i T + c^i P + d^i TP + e^i (P)^2)\,m/s \quad (46)$$

The unknown parameters for each component are tabulated in Table 4.

R-square values in Table 4 are determined by the following equations:

$$R-square^i = 1 - SSR^i/SST^i \quad (47)$$

$$SSR^i = \Sigma_{j=1}^{4}(k_{L_{calculated}}^i - k_{L_{mean}}^i)^2 \quad (48)$$

$$SST^i = \Sigma_{j=1}^{4}(k_{L_{exp}}^i - k_{L_{mean}}^i)^2 \quad (49)$$

Figs. 12 to 15 illustrate the comparison between calculated (from Eq. (4)) and experimental k_L.

The general mass transfer coefficient is determined using Eq. (14). Note that this equation can be converted to the following expression, provided that the difference between experimental and equilibrium pressure is not too large. The benefit of using general mass transfer coefficient is that it is independent of component.

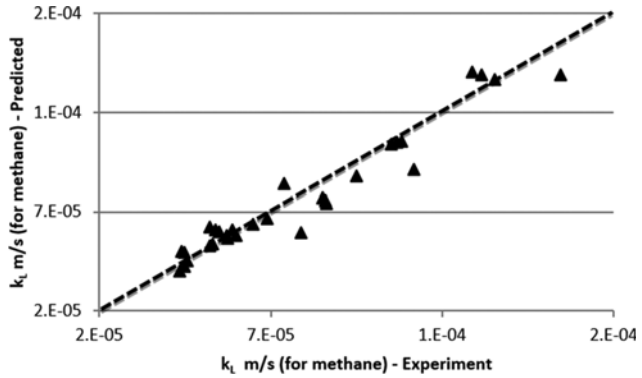

Fig. 12. Comparison between predicted and experimental k_L for methane.

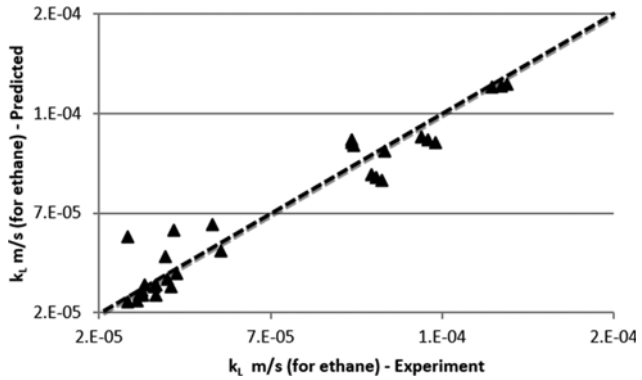

Fig. 13. Comparison between predicted and experimental k_L for ethane.

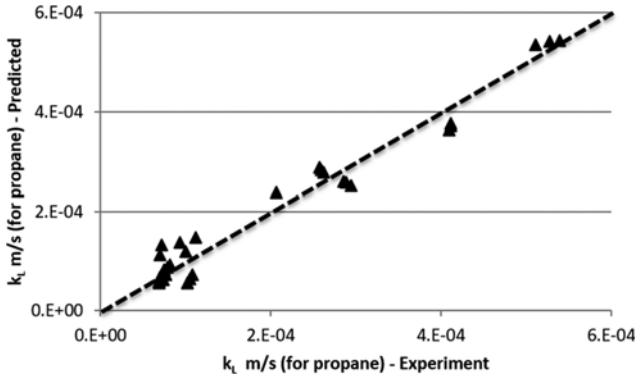

Fig. 14. Comparison between predicted and experimental k_L for propane.

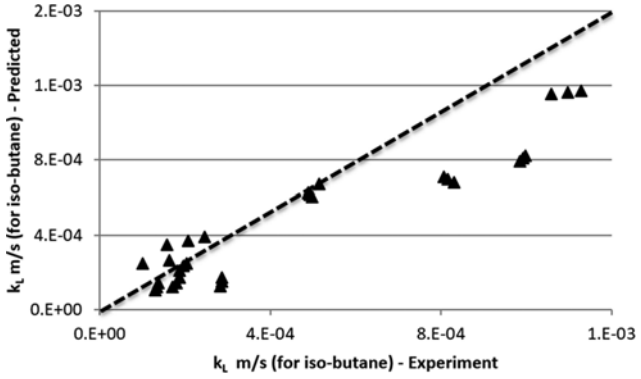

Fig. 15. Comparison between predicted and experimental k_L for i-butane.

Table 5. Parameters of Eq. (51)

a	b	c	d	e	R-square
139.1	−0.5537	18.61	−0.06146	−0.002092	0.97

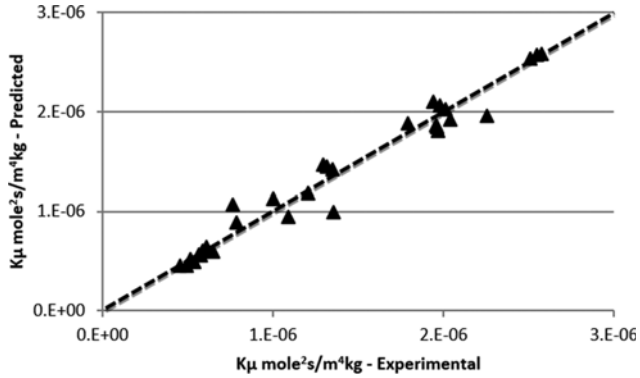

Fig. 16. Comparison between predicted and experimental general mass transfer coefficient-Eq. (51).

$$dn_H/dt = A_{V-L}C_W\Sigma_{i=1}^{m}K_\mu RTy^i/C_W x_{EQ}^i(x^i - x_{EQ}^i) \quad (50)$$

$K_\mu RTy^j/C_W x_{EQ}^j$ part is exactly the component mass transfer coefficient (k_i-see Eq. (4)). A second-order (with respect to pressure) polynomial correlation (Eq. (51)) has been assumed, which its parameters calculated and tabulated in Table 5. A comparison between predicted and experimental values is illustrated in Fig. 16. The absolute average deviation (AAD% - Eq. (52)) of experimental and calculated data (Eq. (51)) is 7.26% which shows acceptable results of the discussed theory.

$$K_\mu = 10^{-7}(a+bT+cP+dTP+eP^2) \quad (51)$$

$$AAD\% = \frac{1}{n}\sum\left|(K_{\mu_{Experimental}} - K_{\mu_{Calculated}})/K_{\mu_{Experimental}}\right| \quad (52)$$

Fig. 17 shows the dependency of K_μ on pressure at different temperatures according to Eq. (51). As was predictable, K_μ is considerably pressure- and temperature-dependent.

From Tables 4 and 5, the component and general mass transfer coefficients decrease with increase in temperature, which seems to be in controversy with molecular diffusion dependency on temperature [34]. This controversy can be explained as follows.

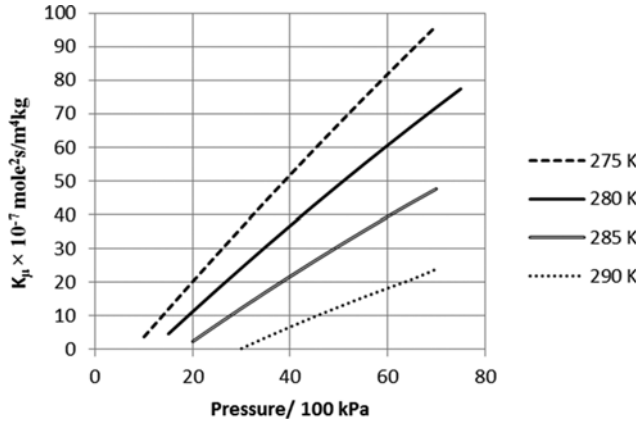

Fig. 17. Dependency of GMC (K_μ) on pressure and temperature.

The calculated k_L and K_μ (in this work) are influenced by two mechanisms, molecular transfer and hydrate formation reaction. Although the molecular diffusion (and consequently mass transfer coefficient) is proportional to temperature, the rise in temperature can reduce the reaction rate. Thus, the calculated mass transfer coefficient has been enhanced by the hydrate formation in the interface of the gas-liquid. As a result, the reported k_L and K_μ can be called enhanced mass transfer coefficients [35], which shows the contribution of hydrate reaction.

CONCLUSION

The current study concentrated on gas hydrate formation from a multicomponent mixture. The chemical potential was introduced as the prime driving force. Several assumptions, including equilibrium and non-equilibrium, were made, and we concluded that the logarithm of the fugacity ratio between experimental and equilibrium conditions can predict the driving force. In addition, the mass transfer approach was used to predict the gas consumption with the hydrate phase. Based on the definition of driving force and the applied approach, a new mass transfer coefficient was introduced. Because the new parameter is independent of the composition and can be employed in a wide range of compositions, it is called the general mass transfer coefficient (GMTC). The dependency of GMTC on the temperature and pressure was experimentally measured and reported. Results showed that the general mass transfer coefficient increases by increasing the pressure and decreasing the temperature.

REFERENCES

1. E. D. Sloan, *J. Chem. Therm.*, **35**, 41 (2003).
2. H. P. Veluswamy, P. S. R. Prasad and P. Linga, *Korean J. Chem. Eng.*, **33**, 1 (2015).
3. A. K. Sum, C. Koh and E. D. Sloan, *Ind. Eng. Chem. Res.*, **48**, 7457 (2009).
4. I. Chatti, *Energy Convers. Manage.*, **46**, 1333 (2005).
5. K. Nazridoust and G. Ahmadi, *Chem. Eng. Sci.*, **62**, 6155 (2007).
6. A. Vysniauskas and P. Bishnoi, *Chem. Eng. Sci.*, **38**, 1061 (1983).
7. P. Englezos and P. Bishnoi, *Chem. Eng. Sci.*, **42**, 2647 (1987).
8. C. Gaillard, J. Monfort and J. Peytavy, International Conference on Natural Gas Hydrates (1996).
9. J. Monfort, *Annals of the New York Academy of Sciences*, **912**, 753 (2000).
10. M. A. Clarke and P. Bishnoi, *Chem. Eng. Sci.*, **60**, 695 (2005).
11. J. Zhang, S. Lee and J. W. Lee, *Ind. Eng. Chem. Res.*, **46**, 6353 (2007).
12. P. Skovborg and P. Rasmussen, *Chem. Eng. Sci.*, **49**, 1131 (1994).
13. D. Kashchiev and A. Firoozabadi, *J. Crystal Growth*, **241**, 220 (2002).
14. C. P. Ribeiro and P. L. Lage, *Chem. Eng. Sci.*, **63**, 2007 (2008).
15. V. Mohebbi, A. Naderifar, R. M. Behbahani and M. Moshfeghian, *Chem. Eng. Sci.*, **76**, 580 (2012).
16. S. Lee, J. Zhang, R. Mehta, T. Woo and W. Lee, *J. Phys. Chem.*, **111**, 4734 (2007).
17. M. K. Chun and H. Lee, *Korean J. Chem. Eng.*, **13**, 620 (1996).

18. M. B. Malegaonkar, P. D. Dholabhai and P. R. Bishnoi, *Canadian J. Chem. Eng.*, **75**, 1090 (1997).
19. S. Bergeron and P. Servio, *Fluid Phase Equilib.*, **265**, 30 (2008).
20. S. Bergeron, J. G. Beltrán and P. Servio, *Fuel*, **89**, 294 (2010).
21. J. Zhang and J. W. Lee, *Ind. Eng. Chem. Res.*, **48**, 5934 (2008).
22. M. Naseh, V. Mohebbi and R. Behbahani, *J. Chem. Eng. Data*, **59**, 3710 (2014).
23. S. Bergeron and P. Servio, *Fluid phase Equilib.*, **276**, 150 (2009).
24. M. Najafi and V. Mohebbi, *J. Nat. Gas Sci. Eng.*, **21**, 738 (2014).
25. A. Izadpand, M. Vafaie and F. Varaminian, *Iranian J. Chem. Chem. Eng.*, **26**, 61 (2007).
26. B. Peng, *J. Phys. Chem.*, **111**, 12485 (2007).
27. S. Babaee, *J. Chem. Therm.*, **81**, 52 (2015).
28. H. Hashemi, *J. Chem. Therm.*, **82**, 47 (2015).
29. R. Christiansen and E. D. Sloan, Gas Processors Association, Tulsa (1995).
30. V. Mohebbi, A. Naderifar, R. M. Behbahani and M. Moshfeghian, *J. Chem. Therm.*, **51**, 8 (2012).
31. G. Soave, *Chem. Eng. Sci.*, **27**, 1197 (1972).
32. A. Danesh, PVT and phase behavior of petroleum reservoir fluids, Elsevier (1998).
33. V. Mohebbi and R. Behbahani, *J. Nat. Gas Sci. Eng.*, **18**, 47 (2014).
34. R. E. Treybal, Mass transfer operations, McGraw Hill (1980).
35. H. S. Fogler, Elements of chemical reaction engineering, Prentice Hall (1999).
36. W. R. Parrish and J. M. Prausnitz, *Ind. Eng. Chem. Process Des. Dev.*, **11**, 26 (1972).
37. Gas Processors and Suppliers Association Engineering Data Book, Tulsa, Oklahoma, U.S.A. (2004).
38. J. Munck, S. Skjold-Jørgensen and P. Rasmussen, *Chem. Eng. Sci.*, **43**, 2661 (1988).

APPENDIX A-ESTIMATION OF EQUILIBRIUM GAS HYDRATE PRESSURE

Van der Waals and Platteeuw [36] introduced the chemical potential of water in hydrate phase (μ^H) by:

$$\mu^H = \mu^\beta + RT\Sigma_{a=1}^{c} v_a \ln(1-\Sigma_{i=1}^{nc}\theta_{ai}) \tag{A1}$$

where, μ^β refers to the chemical potential of water in the hypothetical (empty) hydrate lattice, v_a is the number of cavities of type a per water molecule in the lattice, and θ_{ia} is the fraction of cavities of type a occupied by gas component i. The fractional occupancy is defined by the following Langmuir expression:

$$\theta_{ai} = \frac{C_{ai} f_i}{1+\Sigma_k C_{ak} f_k} \tag{A2}$$

Table 6. Binary interaction of SRK EOS [32]

	Methane	Ethane	Propane	i-Butane
Methane	0	−0.0078	0.008	0.0241
Ethane	−0.0078	0	0	0.001
Propane	0.008	0	0	0
i-Butane	0.0241	0.001	0	0

Table 7. Parameters to estimate the Langmuir constant Eq. (A5) [38]

Cavity	Small		Large	
Name/Parameters	Aij	Bij	Aij	Bij
Methane	0.0002207	3453	0.0076068	1916
Ethane	0	0	0.0040818	2967
Propane	0	0	0.0012353	4638
i-Butane	0	0	0.001573	3800

where, C_{ai} is the Langmuir constant, and f_i is the fugacity of component *i* which is calculated by SRK EOS [31] in this work (Eq. (A3)).

$$f_i = y_i P \varphi_i \tag{A3}$$

with

$$\ln(\varphi_i) = \frac{b_i}{b}(Z-1) - \ln(Z-B) - \frac{A}{B}\left[\frac{2\Sigma_{j=1}^{nc} y_j\sqrt{a_i a_j}(1-k_{ij})}{a} - \frac{b_i}{b}\right]\ln\left(1+\frac{B}{Z}\right) \tag{A4}$$

In the present model, the Langmuir constants are temperature-dependent according to Eq. (A5).

$$C_{ai} = \frac{A_{ai}}{T} e^{\frac{B_{ai}}{T}} \tag{A5}$$

The values of A_{ai} and B_{ai} are reported in Table 7. On the other hand, the difference in chemical potential of water in the empty hydrate lattice and that in the pure liquid state at the system temperature and equilibrium pressure is:

$$\frac{\mu^\beta - \mu^0}{RT} = \frac{\Delta\mu_0}{RT} - \int_{T_0}^{T}\frac{\Delta h}{RT^2}dt + \int_0^P \frac{\Delta v}{RT}dT \tag{A6}$$

$$\Delta h = \Delta h^0 + \int_{T_0}^{T}(\Delta C_P^0 + \beta(T-T_0))dT \tag{A7}$$

The values of $\Delta\mu_0$, Δh, Δv, ΔC_P^0, and β are listed in Table 8 for the hydrate structure II. At equilibrium conditions, the chemical potential of water in hydrate and pure water is equal. Thus, the combination of Eqs. (A6) and (A7) gives:

$$\frac{\Delta\mu_0}{RT} - \int_{T_0}^{T}\frac{\Delta h}{RT^2}dt + \int_0^P \frac{\Delta v}{RT}dT = -\Sigma_{a=1}^{c} v_a \ln(1-\Sigma_{i=1}^{nc}\theta_{ai}) + \ln\gamma_W x_W \tag{A8}$$

$\mathrm{Ln}(\gamma_W x_W)$ is added to Eq. (A8) to consider the effect of non-ideality of water phase. This term can be omitted as the hydrocarbon

Table 8. Values for thermodynamic reference parameters of structure II of gas hydrates [38]

Parameter	Value	Unit
$\Delta\mu_0$	J/mole	883
Δh	J/mole	−5203.5
Δv	m^3/mole	3.4×10^{-6}
ΔC_P^0	J/mole.K	−38.13
β	J/mole·K^2	0.141

components dissolution in water is negligible. The above equation is a non-linear equation that should be solved to calculate the equilibrium pressure. Newton-Raphson method was used to evaluate the equilibrium pressure. The initial pressure guess was estimated, using distribution coefficient method [37].